Z. Dt. Ges. Geowiss. (J. Appl. Reg. Geol.), **172 (3)**, p. 293–305, 6 figs.
Published online September 2021

Article
Open Access

Modelling the 3D geometry of the Dinantian carbonate geothermal reservoir in northern France

Aurore Laurent[1], Laurent Beccaletto[2], Olivier Averbuch[1], Fabien Graveleau[1], Frédéric Lacquement[2], Séverine Caritg[2], Stéphane Marc[2] & Laure Capar[2]*

Laurent, A., Beccaletto, L., Averbuch, O., Graveleau, F., Lacquement, F., Caritg, S., Marc, S. & Capar, L. (2021): Modelling the 3D geometry of the Dinantian carbonate geothermal reservoir in northern France. – Z. Dt. Ges. Geowiss., 172: 293–305, Stuttgart.

Abstract: The current research project aims at better characterising the 3D geometry of the main deep geothermal reservoir in northern France: the Dinantian karstic and brecciated limestones (lower Carboniferous, Mississippian). The detailed 3D geometry of this buried reservoir in the region has been investigated here through the integration of a large database including 1,128 boreholes and 532 km of reprocessed and interpreted seismic reflection profiles. This geological information was then interpolated in a 3D structural model using the GeoModeller software. Despite residual uncertainties related to the time-depth conversion procedure of the seismic data as well as the interpolation process, it provides an image of the 3D geometry of the Dinantian sequence at depth with an unprecedented resolution.

The 3D modelling indicates that the Dinantian reservoir is rather continuous and extends over an area of approximately 7,675 km² in northern France-southwestern Belgium. Interestingly, we document that the Dinantian reservoir extends at least 30 to 40 km south or southwest of the coal basin area as indicated by the geometry of its cut-off line with the major frontal and lateral ramps of the Allochthon Main Basal Thrust of the Northern Variscan Front. From the Lille metropolitan area, where the Dinantian is rather shallow (depth lower than 200 m), the Dinantian reservoir strongly deepens southward as it reaches 1,000–3,000 m depth beneath the coal basin district and a maximum depth of about 7,000 m at the southern end of the study area.

Keywords: 3D structural modelling, Dinantian geothermal reservoir, Northern Variscan thrust front

1. Introduction

Over the last few decades, growing societal awareness regarding the need to turn to renewable energies has led to the implementation of new energy policies. Following the Paris Agreements for climate change in 2015, governments are committed to massively invest into and develop renewable energies in the coming decades. Among this renewable energy package, geothermal energy is probably one of the less known, although it is locally of major importance. Numerous projects for the development of deep geothermal energy have thus been launched recently both at the European level, such as the Interreg North-West Europe DGE-ROLLOUT project, and at the regional scale, e.g. the Hauts-de-France region in northern France.

In the Hauts-de-France region (northern France), the populated Nord-Pas-de-Calais (NPC) coal basin district (1.5 million inhabitants), located above the fossil deformation front of the Variscan Orogen, constitutes an interesting target for the development of low-temperature deep geothermal energy. Such orogenic fronts have long been favoured targets for the exploration and exploitation of hydrocarbons and coal. It was particularly the case of the NPC Molasse foreland basin explored and exploited for coal production during the 19th–20th centuries. More recently, however, they have raised major interest for deep geothermal applications. Indeed, in such geological setting, potential rock reservoirs can be buried at a few kilometres depth beneath the foreland basin, thereby creating favourable conditions for the generation of high-temperature waters. This is, for example, the case in Bavaria, Germany, near Munich, where high-temperature geothermal fluids (80–140 °C) are extracted beneath the Alpine molassic basin (Farquharson et al. 2016).

In late Carboniferous times, the development of the Variscan NPC Molasse foreland basin led to the burial of the pre-orogenic sequence up to few kilometres depth in northern France; the region-wide Dinantian (Lower Carboniferous) carbonate units are part of this buried pre-orogenic se-

*Addresses of the authors:
[1]Univ. Lille, CNRS, Univ. Littoral Côte d'Opale, UMR 8187 – LOG – Laboratoire d'Océanologie et de Géosciences, F-59000 Lille, France (aurore.laurent@univ-lille.fr / olivier.averbuch@univ-lille.fr / fabien.graveleau@univ-lille.fr)
[2]BRGM, F-45060 Orléans, France (l.beccaletto@brgm.fr / f.lacquement@brgm.fr / s.caritg@brgm.fr / s.marc@brgm.fr / l.capar@brgm.fr)

DOI: 10.1127/zdgg/2021/0284
E. Schweizerbartsche Verlagsbuchhandlung, Stuttgart, Germany, www.schweizerbart.de

quence. Due to their highly fractured and karstified character, they constitute the main target reservoir for the exploitation of deep geothermal energy in northern France. This reservoir is already exploited in Belgium in the Hainaut coal district area, that is the eastward prolongation of the NPC coal district area, where the water temperature in the three geothermal wells of Douvrain, Ghlin and Saint-Ghislain reaches 60–70 °C (e.g. Delmer 1982; Licour 2012). In northern France, the Dinantian reservoir has only been observed through boreholes and its geothermal potential is not well constrained. A few geothermal anomalies have been recorded in the NPC coal basin district at the source of Saint-Amand-les-Eaux (23 °C) and near Lens in the mining boreholes of Lens n°10 and Meurchin n°2 (40 °C at 240–335 metres depth; Becq-Giraudon 1983). During the 1980s, a geothermal exploration well was drilled at Condé-sur-l'Escaut, less than 20 kilometres from the Belgian productive geothermal wells, without finding any geothermal evidence. This highlighted the geographical variability of the geothermal potential in the region, most probably related to both the hydrodynamics within the Dinantian reservoir and the complex structure and fault network along the Northern Variscan Front.

In this general context, our study aims at defining the 3D geometry of the buried Dinantian carbonate reservoir in northern France. It is based on the 3D modelling of the structure of the Northern Variscan Front in northern France–southwestern Belgium, using the GeoModeller software. This 3D model integrates a large database, comprising 532 kilometres of reprocessed seismic reflection profiles, 1,128 boreholes as well as local structural data. A depth structural map of the top of the Dinantian reservoir in the study area has been generated as a result of the modelling process. This 3D modelling approach allows defining the extension and depth of the Dinantian carbonate reservoir with an unprecedented resolution and thereby represents the first step towards assessing the geothermal potential in the region.

2. Geological setting

2.1 The Dinantian carbonate sequence in northern France

In NW Europe, the Dinantian carbonate units (Lower–Middle Mississippian, 359–331 Ma) are known all around the lower Palaeozoic London-Brabant Massif. They extend from Ireland via England to the Netherlands and from northern France via Belgium to western Germany (Arndt 2021; Broothaers et al. 2021; Pharaoh et al. 2021; Pracht et al. 2021). In northern France, the Dinantian units and the entire Palaeozoic substratum are generally covered, unconformably, by a 100–200 metres thick Cretaceous-Tertiary sequence, deposited along the northern border of the Paris Basin (Fig. 1). The Dinantian sequence is thus mainly constrained through boreholes (see reference wells in Fig.2a), and on a few outcrops localised in the Boulonnais (English Channel borders) and Avesnois regions (western end of the Ardennes Massif) as well as in the Mons-Tournai area (southwestern Belgium) (Fig. 1).

In the NPC coal district area (northern France) and in the Hainaut region (southwestern Belgium), the known thickness of the complete Dinantian series varies between 600 m in the area of Jeumont (COPESEP 1965) and 2,600 m in the area of Saint-Ghislain (Groessens et al. 1982). The lower Dinantian or Tournaisian (Lower Mississippian, 359–347 Ma), is well documented in the boreholes Tournai, Vieux-Leuze (Coen-Aubert et al. 1980) and Saint-Ghislain (Groessens et al. 1982) (Fig. 2a). It consists of shales, calcareous shales with crinoidal beds and crinoidal limestones with argillaceous intervals and cherty layers (Poty et al. 2001; Hance 2006a) (Fig. 2c). At its base, the uppermost Devonian-lowermost Tournaisian is characterised by sandstones, dolomitic sandstones, shales, dolomitic limestones and sandy limestones. The upper Dinantian or Visean (Middle Mississippian, 347–331 Ma) consists mostly of bioclastic and crinoidal dolomites and limestones. It usually comprises thick intervals of brecciated limestones with stromatolitic levels (Groessens et al. 1982; Poty et al. 2001; Hance et al. 2006b; Fig. 2c). The extensive brecciated character of the Visean limestones is attributed to the polyphased, long-term dissolution of interstratified evaporite sequences during the successive events of burial of the Dinantian rocks (Rouchy et al. 1986, 1987; De Putter 1995; De Putter et al. 1994). Thick residual levels of anhydrite are locally preserved in the Visean series of the Epinoy and Saint-Ghislain boreholes (Delmer 1977; Rouchy et al. 1986, 1987; De Putter et al. 1991, 1994); where anhydritic levels are present, brecciated limestones are more scarce (Licour 2012). The heterogeneity and fractured character of the Visean brecciated limestone sequence together with its higher tendency for local karstification make this unit the main geothermal target in the N France-Hainaut area.

From a palaeogeographical point of view, the Dinantian series of northern France (Lille and NPC coal district area) and southwestern Belgium (Mons-Tournai area) were deposited in a marine shallow-water carbonate environment at the southern margin of the Laurussian continental block. Overall, it evolved from a south-facing ramp in the early Tournaisian to a rimmed shelf during the late Tournaisian-early Visean (Hance et al. 2001, 2006a; Poty et al. 2001). During the mid–late Visean, this carbonate sequence deposited on a broad shelf of regional extent. A polarity inversion occurred in the middle Visean (Livian): facies characteristics of a more restricted marine environment (e.g. anhydrite, stromatolitic facies) deposited to the south while open marine facies deposited to the north (Hance et al. 2001, 2006b; Poty et al. 2001). This change reflects the first effects of the northward propagating uplift associated to the tectonic inversion of the Laurussian margin and the subsequent development of the Variscan thrust front.

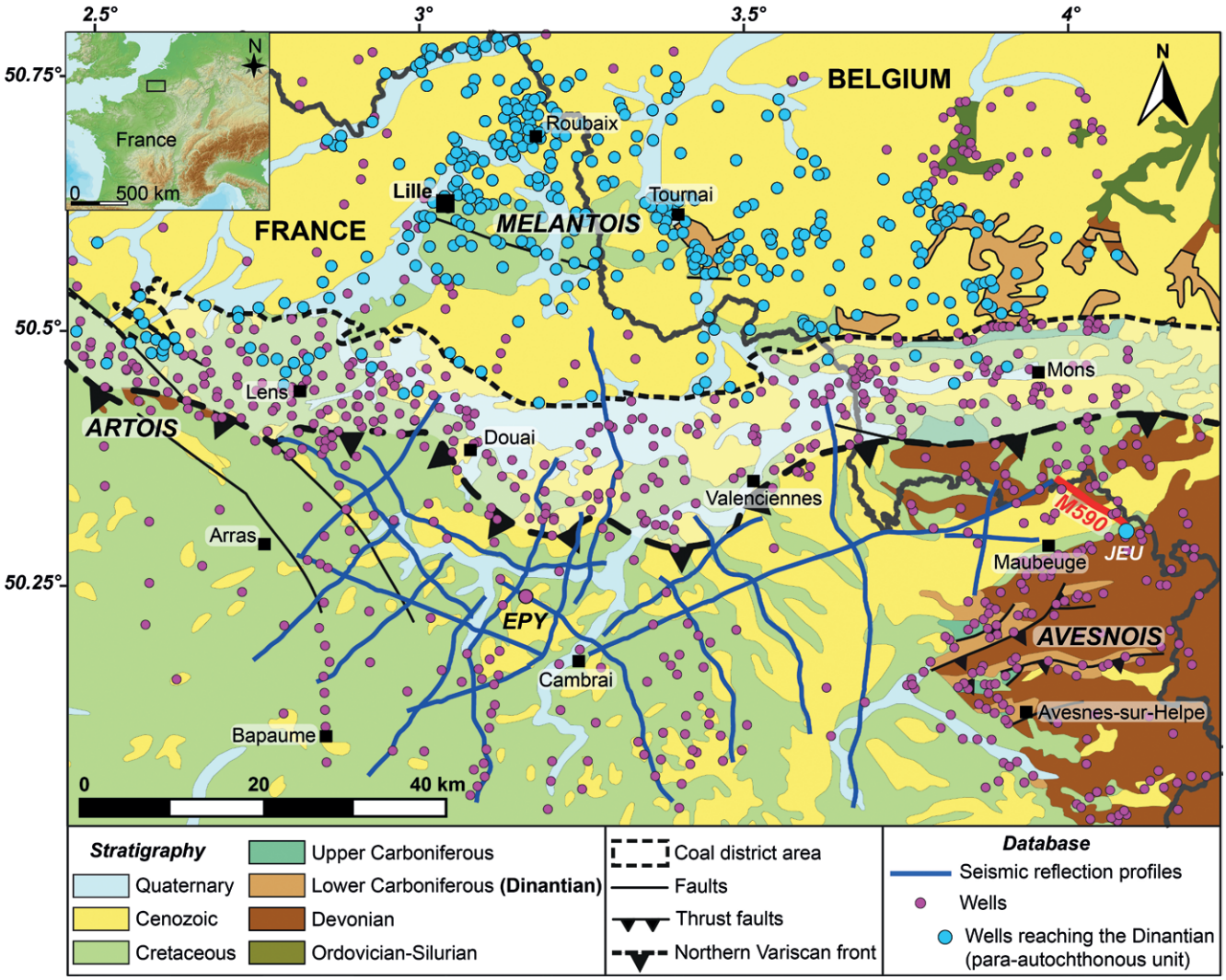

Fig. 1: Simplified geological map of the modelled area extracted from the geological map of France (Chantraine et al. 2003) reporting the location of the boreholes and seismic reflection profiles used to produce the 3D model. Dinantian outcrops in the Brabant Para-autochthonous Unit (Belgium) have been delimited by a thick black line. Borehole legend: EPY – Epinoy; JEU – Jeumont.

2.2 Structural framework

The Dinantian units developed as part of a large-scale post-rift transgressive carbonate platform onto the slowly subsiding southern Laurussian margin from the late Eifelian to the Visean (Meilliez et al. 1991; Mansy et al. 1999). This large platform recorded the long-term thermal subsidence of the proximal southern margin of the Laurussian continent following a major rifting phase that took place from Early (Lochkovian) to Middle Devonian (Eifelian) (Meilliez et al. 1991; Franke 2000; Shail & Leveridge 2009). This rifting event triggered the opening of the Rheno-Hercynian Ocean in between the northern Laurussian margin and the southern Armorica-Saxo-Thuringia continental blocks. The syn-rift subsidence of the Laurussian margin was marked by normal faulting oriented along two main directions: i.e. N50-70° and N110-130° (Meilliez et al. 1991).

From Late Devonian times onward, tectonic kinematics changed and the subsequent N–S convergence between Avalonia and the Armorica-Gondwana accretion complex led to the progressive southward subduction and closure of the Rheno-Hercynian Ocean and to the collision of the surrounding margins during the middle Visean (ca. 340 Ma; Cazes et al. 1985; Averbuch & Piromallo 2012 ; Franke et al. 2017). This Variscan collision stage, characterised by an overall NNW–SSE shortening, lasted about 35 Ma until the Middle Pennsylvanian (ca. 305 Ma) and led to the gradual tectonic inversion of the southern Laurussian margin (e.g. Oncken et al. 1999, 2000; Averbuch et al. 2004; Averbuch & Piromallo 2012). It resulted in the development of a north-vergent thrust system extending in northern France from the Channel borders (Boulonnais) to the Avesnois region (Maubeuge area in Fig. 2; Cazes et al. 1985; Raoult & Meilliez 1987; Averbuch et al. 2004).

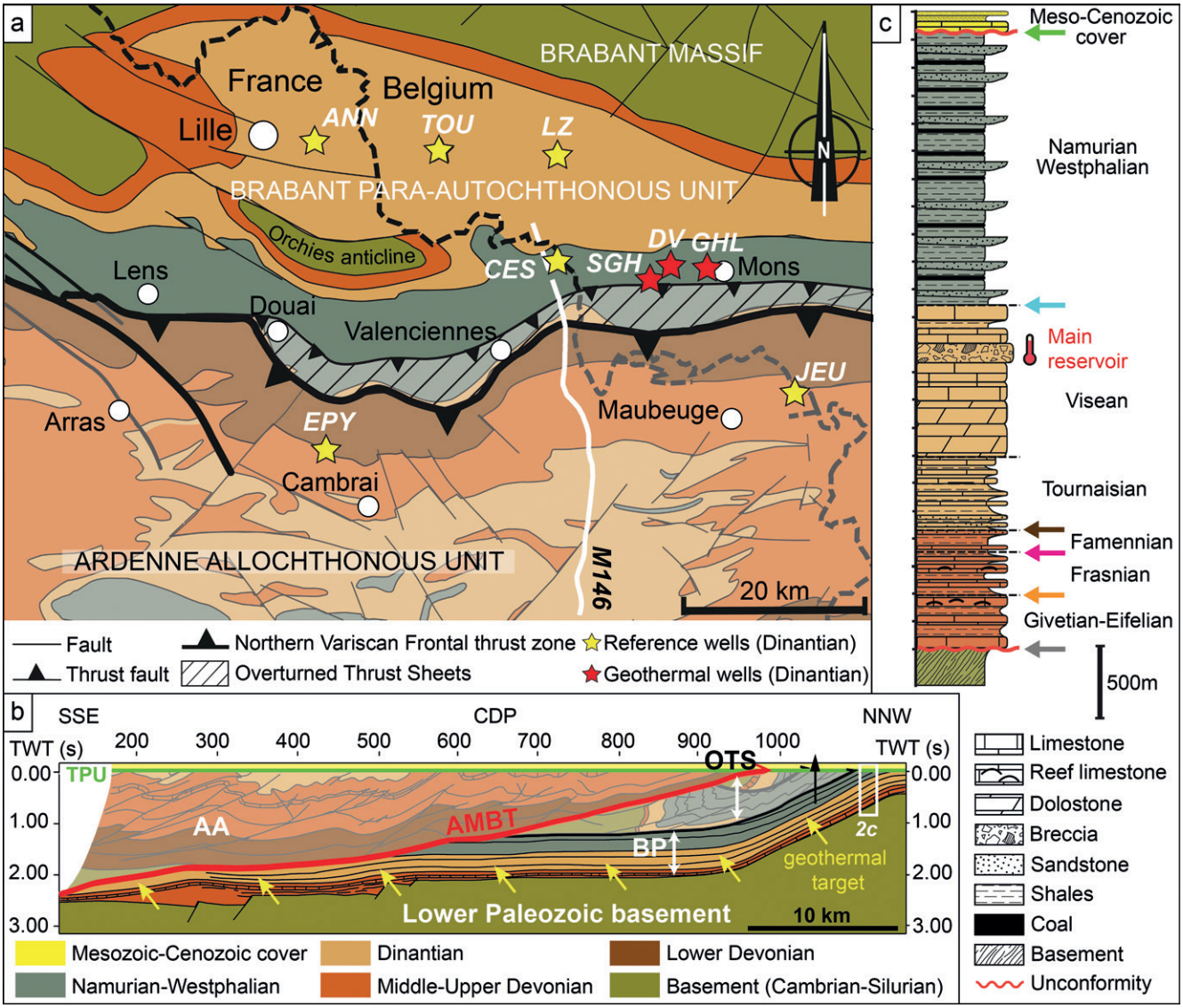

Fig. 2: (**a**) Structural map of the Variscan basement in the modelled area (modified from CFP et al. 1965 and Averbuch et al. 2004). Only the geological levels modelled in 3D are represented in full colours (i.e. Brabant Para-autochthonous Unit). The reference wells correspond to the deep boreholes used to define and describe the Dinantian in northern France-southwestern Belgium. Borehole legend: ANN – Annappes; CES – Condé-sur-l'Escaut; DV – Douvrain; EPY – Epinoy; GHL – Ghlin; JEU – Jeumont; LZ – Leuze; SGH – Saint-Ghislain; TOU – Tournai. (**b**) Interpretation of the M146 seismic profile (location in Fig. 2a), illustrating the structure of the Northern Variscan Front in the area of Valenciennes (modified from Lacquement et al. 1999 and Mansy & Lacquement 2006). AA – Ardennes Allochthonous Unit; AMBT – Allochthon Main Basal Thrust; BP – Brabant Para-autochthonous Unit; OTS – Overturned Thrust Sheets; TPU – Top Palaeozoic Unconformity. (**c**) Synthetic lithostratigraphic log of the Brabant Para-autochthonous Unit in northern France-southwestern Belgium. Indicated thicknesses have been defined based on the data of the reference boreholes in the region (Fig. 2a). The coloured arrows point at the geological surfaces interpreted in seismics (Fig. 3) and modelled in 3D. Main Dinantian geothermal reservoir is indicated.

The Dinantian carbonate units of northern France were primarily deformed during the Variscan orogenic cycle. Subsequent deformation events (i.e. the late Carboniferous-Permian and Late Jurassic-Early Cretaceous rifting episodes as well as the Tertiary inversion related to the far-field accommodation of the Alpine-Pyrenean shortening) produced only second-order structures, mostly localised along the Artois-Boulonnais hills (western limit of the area under study) and the Mélantois dome (between Lille and Tournai) (e.g. Mansy et al. 2003; Minguely et al. 2010 and references herein). Beneath the Mesozoic-Cenozoic cover, the Dinantian series are incorporated within three major structural units involved in the northern Variscan thrust front (from north to south): the Brabant Para-autochthonous Unit, the Overturned Thrust

Sheets and the Ardennes Allochthonous Unit (Fig.2a; Meilliez & Mansy 1990; Mansy et al. 1997, 1999; Lacquement et al. 1999).

The Brabant Para-autochthonous Unit corresponds to the slightly deformed part of the Laurussian continental margin. It is formed by the Middle Devonian to lower Carboniferous (late Eifelian–Visean) post-rift transgressive cover of the Brabant lower Palaeozoic basement and by the overlying synorogenic molasse (Fig. 2c), deposited along the Northern Variscan foredeep during the Late Mississippian-Middle Pennsylvanian (Namurian–Westphalian, 325–305 Ma; Fig. 2a). In northern France, this basin, known as the NPC coal basin, involves an up to 3.5 km thick molasse sequence made of an alternation of fluvio-deltaic and paralic deposits (Bouroz 1969; Becq-Giraudon 1983; Delmer et al. 2001). This structural unit displays an overall monoclinal geometry with a general gentle southward dip (5–10°; Fig. 2b) due to the flexural response of the foreland to thrust loading. North of the emergence of the frontal thrust zone, it displays however a major flexure allowing for the exhumation of the Palaeozoic substratum directly below the Mesozoic-Cenozoic cover (the Orchies anticline in Fig. 2a).

To the south, the Brabant Para-autochthonous Unit is overthrust by the Ardenne Allochthonous Unit along a major crustal-scale thrust zone (Figs. 2a, b; Raoult 1986; Meilliez & Mansy 1990; Mansy et al. 1997; Lacquement et al. 1999). The latter is referred to, in this paper, as the Allochthon Main Basal Thrust (AMBT). Its emerging part, which delimits the southern extension of the coal district area, is usually known as the Midi Fault (Meilliez 2019 and references herein). The Ardenne Allochthonous Unit is composed of a more complete and thicker Lower Devonian to Dinantian sequence than the Brabant Para-autochthonous Unit due to its more distal palaeogeographic position on the southern Laurussian margin. The allochthonous unit forms part of a typical fold-and-thrust belt with an overall E–W to ENE–WSW trend in the area under study (Khatir et al. 1988; Meilliez & Mansy 1990; Mansy & Meilliez 1993; Lacquement 2001; Moulouel 2008). In northern France, restoration of the margin geometry before compression suggests that the Ardenne Allochthonous Unit was displaced over at least 60–70 km northward along the main frontal thrust zone (Raoult & Meilliez 1987; Lacquement et al. 1999; Mansy et al. 1999; Laurent et al. 2021). This intense deformation is emphasised by the existence of thrust sheets characterised by a complex and overall overturned geometry between the Brabant Para-autochthonous Unit and the Ardenne Allochthonous Unit (Bouroz et al. 1961; Delmer 1997, 2003; Mansy et al. 1997; Lacquement et al. 1999; Fig. 2b). These so-called "Overturned Thrust Sheets" (OTS) consist of a folded Silurian to upper Carboniferous sequence affected by a series of second-order NNW-vergent forelimb thrusts (Bouroz 1950; Le Gall 1994; Meilliez 2019). This typical structural style is depicted in the N–S cross-section of Fig. 2b, based on the interpretation of the reference M146 seismic profile in the Valenciennes area (Mansy et al. 1997; Lacquement et al. 1999; Laurent et al. 2021).

3. Data and methodology

3.1 Selection of the seismic and well data

The 3D geometry of the Dinantian carbonate reservoir in the NPC coal district area and its southward extension below the Ardenne Allochthonous Unit has been investigated by modelling the 3D structure of the Northern Variscan Front in northern France and southwestern Belgium (Hainaut area). The study area extends over 125 km E–W, from the Hainaut coal basin district in the east to the Artois region in the west, and over 86 km N–S, from the northerly Roubaix-Tourcoing cities to the southern limit of the Nord-Pas-de-Calais region (Fig. 1). It represents a surface area of 10 750 km^2.

A large database including mainly seismic reflection and well data was compiled prior to the 3D modelling process. 21 seismic reflection profiles, acquired during the onshore oil exploration of the northern Paris Basin (France) in the 1980s, have been reprocessed by the BRGM–French Geological Survey (static corrections, velocity analysis, noise attenuation, pre-stack time migration) and interpreted within the scope of this study (Fig. 1). Given the acquisition parameters used in the surveys (recording length up to 5 seconds two-way-time), the estimated depth of investigation is around 7 to 8 km and the vertical resolution of seismic imaging is approximately 25–30 metres. Seismic lines represent a total length of 532 km and cover an area of approximately 5,130 km^2 over the allochthonous and para-autochthonous units (Fig. 1). The seismic profiles cross the region along various orientations allowing their interpretation to provide an updated image of the 3D structure of the Dinantian carbonate platform in the investigated area. The seismic interpretation was carried out using the IHS Kingdom Software. The targeted geological surfaces have been identified in seismics by calibrating and tying seismic and well data. Synthetic seismograms have been produced using the velocity data from the Epinoy and Jeumont boreholes (Fig. 1), which are the only wells of sufficient depth in the vicinity of the seismic lines to cross the targeted geological levels (see the example of the seismic-well tie between the Jeumont borehole and the M590 seismic profile in Fig. 3a). Several geological horizons and faults have been interpreted (Fig. 2c), with a special focus on the Dinantian carbonates and the regional structural pattern (see Laurent et al. 2021 for further details).

In addition to the seismic data, 1,128 boreholes reaching the Palaeozoic basement have been selected in northern France and southwestern Belgium and included in the database (Fig. 1). A methodical screening process limited to one borehole in a 500 m radius was applied in order to collect as much relevant well data as possible, while avoiding redundant and excessive information. Among the 1,128 selected boreholes, 389 reach the Dinantian in the Brabant Para-autochthonous Unit (Fig. 1). All but one (Jeumont) of these boreholes are located north of the Variscan front. South of the Variscan front, where the underthrust Dinantian units deepen below the thick Ardenne Allochthonous Unit, only the seismic data provides information at

depth, thus reflecting the complementarity of seismic and well data (Fig. 1).

Finally, our database was completed with structural data from the geological maps of France (1: 1,000,000; Chantraine et al. 2003) and Wallonia (Belgium) (1: 25,000, "Carte géologique de Wallonie", Programme de révision de la Carte géologique de Wallonie), such as azimuth and dip values and stratigraphic contacts (see the Dinantian outcrops highlighted in Fig. 1). A digital elevation model (DEM) with a resolution of 25 metres (EU-DEM v1.1 from the Copernicus Land Monitoring Service), provided the required topographic information (Fig. 4).

3.2 Time-depth conversion of the seismic data

Seismic horizons interpreted in time (Fig. 3a) have been converted to depth before being integrated into the 3D model. To do so, several time-depth (TD) conversion methods have been tested: (1) time-depth conversion using the seismic stacking velocities, obtained from the reprocessing of the seismic profiles in time; (2) time-depth conversion based on the migration velocities used for the pre-stack depth migration (PSDM) of six seismic profiles, carried out as part of the Interreg North-West Europe DGE-Rollout project; and (3) layer-cake time-depth conversion using interval velocities obtained from well data.

The accuracy of the different methods could only be checked and compared at the very few wells located in the vicinity of the seismic lines and deep enough to cross the geological surfaces of interest, particularly the Epinoy and Jeumont boreholes (Fig. 1). This relatively limited well control constitutes the main limitation of this procedure.

After comparing the results of all three methods, the layer-cake TD conversion was chosen to maintain 3D consistency between the profiles and the well data. This method is based on the principle that a constant velocity is attributed to each layer displaying similar velocity behaviour (Marsden 1989). The velocity behaviour is defined by lithologies and rock properties and the interval velocity of a given layer corresponds to the mean velocity within this layer:

$$V_{int} = \frac{Z_{base} - Z_{top}}{OWT_{base} - OWT_{top}} \quad \text{Eq. 1}$$

with OWT = one-way time, Z = depth.

We therefore considered every geological level of the stratigraphic pile of the model (see 3.1) as a distinct layer with a constant interval velocity in the entire study area (Fig.

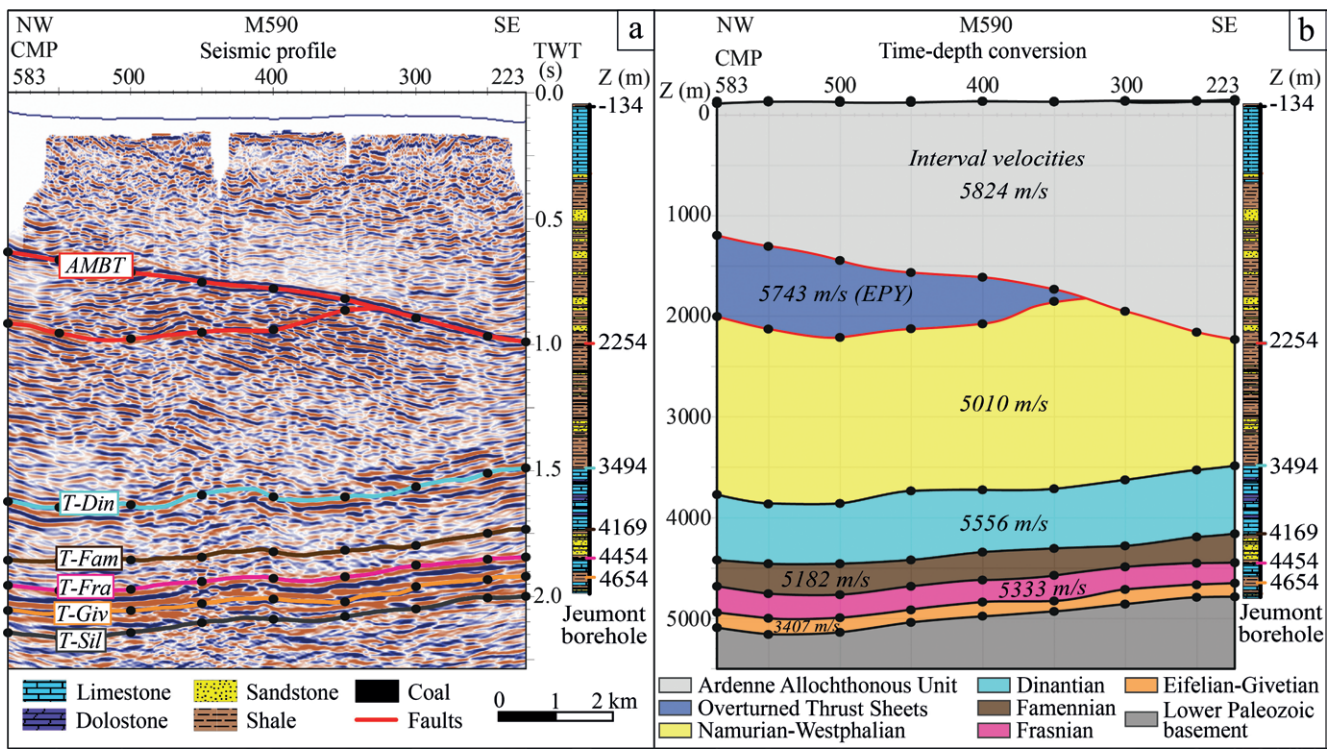

Fig. 3: (**a**) Geological interpretation of the M590 seismic reflection profile. The profile is highlighted in red in Fig. 1. The Jeumont borehole has been tied to the seismic line by generating a synthetic seismogram using well log data (Sonic log). The black dots show the time data points converted in depth using the interval velocities. AMBT – Allochthon Main Basal Thrust; T-Din – Top Dinantian; T-Fam – Top Famennian; T-Fra – Top Frasnian; T-Giv – Top Givetian; T-Sil – Top Silurian. (**b**) Time to depth conversion of the M590 seismic reflection profile using the interval velocities of the Jeumont borehole. Note that the interval velocity of the Overturned Thrust Sheets comes from the Epinoy borehole (EPY).

3b). The interval velocities in the Brabant Para-autochthonous Unit and in the Overturned Thrust Sheets have been computed from the data of the only two wells crossing these units, respectively the Jeumont and Epinoy boreholes (Fig. 1). The interval velocity in the Ardenne Allochthonous Unit corresponds to a mean value calculated from the data of both wells. Finally, to ensure a better geological consistency, a different interval velocity in the Mesozoic-Cenozoic cover has been computed for each line, using the data from nearby boreholes. The interpreted seismic horizons have then been converted to depth step by step from the shallowest (base of the Meso-Cenozoic cover) to the deepest one (top of the lower Palaeozoic basement), using a sampling rate of 50 CMP (common midpoint) (i.e. every 1,250 metres) along each seismic profile. Fig. 3b illustrates an example of TD conversion of the M590 profile, close to the Jeumont borehole.

Like any other TD conversion method, the layer-cake TD conversion has some limitation. First, because the interval velocities are computed based on the data of only two boreholes, the TD conversion of the seismic profiles does not take into account the potential lateral variations of lithologies and rock properties. Therefore, uncertainties increase as distance from the reference boreholes increases. However, considering the lithologies described in the boreholes, the facies variations are very likely not significant enough at the regional scale to have a major impact on the velocity behaviour of the different units.

3.3 3D modelling workflow

The 3D modelling of the Dinantian carbonate reservoir was carried out using the GeoModeller software developed by the French Geological Survey (BRGM) and Intrepid Geophysics Company (www.intrepid-geophysics.com). The modelling method used in this software, referred to as the "potential-field method" (Lajaunie et al. 1997), was specifically designed to compute the geological surfaces and volumes based on both stratigraphic contact points and orientation points (azimuth, dip and polarity values) from geophysical, structural and well data (Fig. 4). It uses a cokriging algorithm to interpolate a 3D potential-field scalar function describing the geology of the study area (Lajaunie et al. 1997; Chilès et al. 2004; Aug et al. 2005; McInerney et al. 2005; Calcagno et al. 2008; Maxelon et al. 2009).

A stratigraphic pile incorporating the main regional geological levels has been established in order to best define the 3D structure of the Northern Variscan Front. Each geological formation of the stratigraphic pile has been assigned to a rule, either "Erode" or "Onlap", defining its relationship with older formations. The stratigraphic column includes from base to top: The lower Palaeozoic basement (onlap), the Middle Devonian (erode), the Frasnian (onlap), the Famennian (onlap), the Dinantian (onlap), the Namurian-Westphalian (onlap), the OTS (erode), the Ardenne Allochthonous Unit (erode) and the discordant Mesozoic-Cenozoic cover (erode) (see Figs. 2b, c). By defining the stratigraphic pile and the relationship rules, the geological history of the study area is automatically taken into account during the modelling process, making it easy to try out different interpretations.

Once the stratigraphic pile of the model was created, the input database described above (3.1) was integrated to the GeoModeller Software (Fig. 4). The fault network and the fault interactions with the different series have been established using the specific features of the GeoModeller software. Stratigraphic horizons and faults were then modelled step by step so that they match structural, seismic and well data. In areas where the geometry of the modelled surfaces was geologically inconsistent, especially in areas with no or insufficient data, 3D construction points were added to the dataset on horizontal and vertical cross-sections. This ensured the 3D structural consistency of the model. At the end of the modelling process, depth structural maps have been extracted from the model using a grid cell size of 250 m (Fig. 4).

4. 3D geometry of the top of the Dinantian carbonate reservoir: results and discussion

The 3D geometry of the Dinantian carbonate reservoir in northern France-southwestern Belgium is presented in this paper through the detailed analysis of the 2D depth structural map of the top of the Dinantian limestones (Fig. 5). It is important to notice that the top of the Dinantian unit is of variable geological nature (domains [a], [b] and [c] in Fig. 5 inset) from south to north. The top Dinantian corresponds to the stratigraphic Dinantian-Namurian boundary in domain [b], it is a truncation limit southward in domain [a] and an erosive limit northward in domain [c]. To the south, the truncation limit corresponds to the tectonic contact between the Dinantian and the overthrusting Ardennes Allochthonous Unit, i.e. the AMBT. To the north, the top limit of the Dinantian series is eroded and truncated by the discordant Mesozoic-Cenozoic cover. Thereby, north of the truncation line (domain [c] in Fig. 5), the modelled geological surface represents the Dinantian-Cretaceous unconformity or Top Palaeozoic Unconformity (TPU).

In the study area, the Dinantian sequence extends over a surface area of approximately 7,675 km^2 (Fig. 5). Interestingly, it extends at least 30 to 40 kilometres south of the coal district area beneath the Ardenne Allochthonous Unit. Additionally, the Dinantian sequence is absent west of Arras, because it is truncated in the Artois region by the lateral ramp of the AMBT. The few tightened contour lines south of the cutoff line indicate a stronger dip of the truncated top of the Dinantian unit and therefore of the AMBT. These observations corroborate previous studies (Minguely 2007), showing that the main frontal thrust is steeper in the Artois region (20°) than in the NPC coal basin area (5–10°). To the north, beneath the unconformable Mesozoic-Cenozoic cover (area [c] in Fig. 5), the Dinantian extends beyond the Roubaix and Tournai cities and edges the Brabant Massif in Belgium.

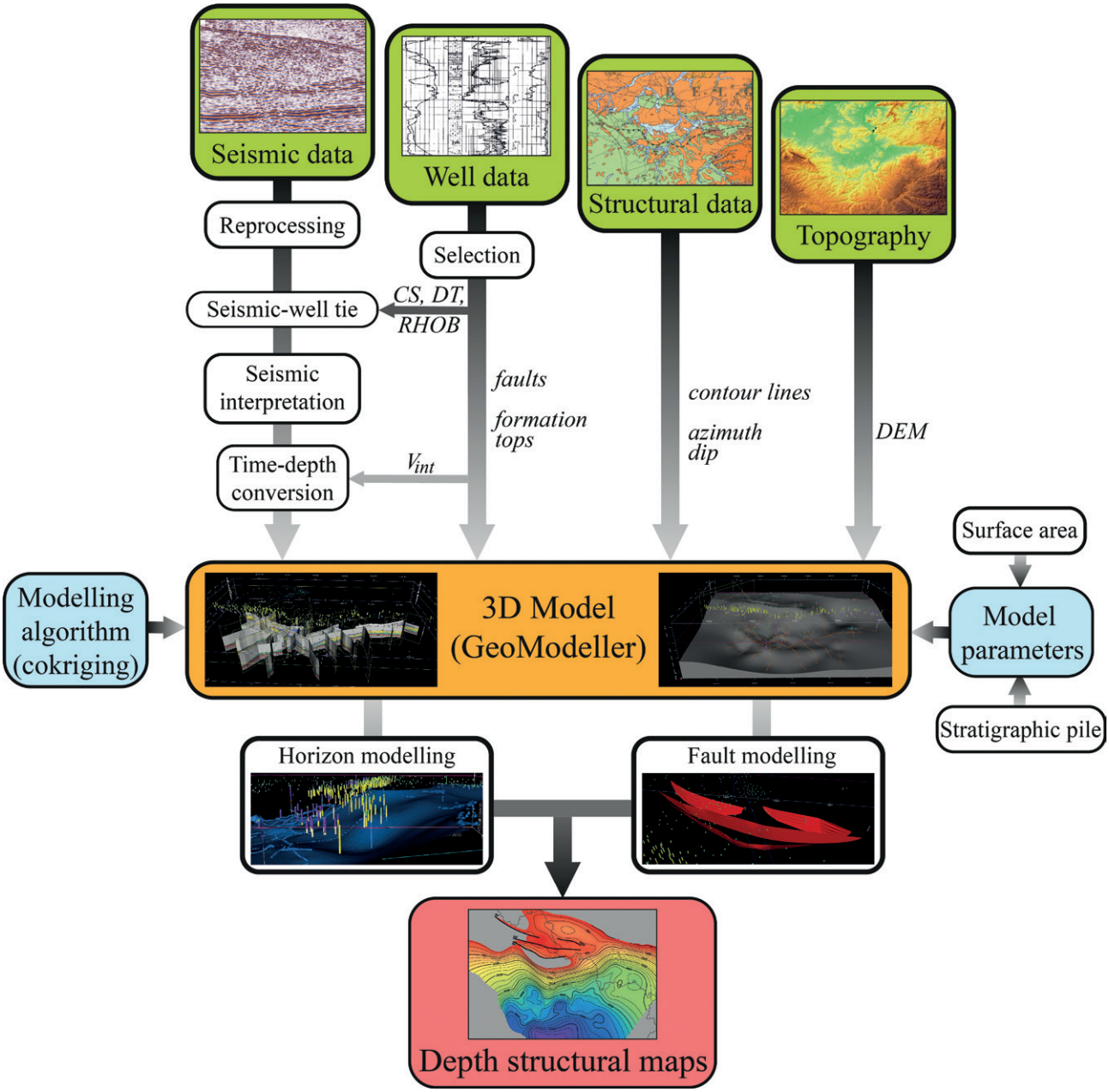

Fig. 4: Flow chart of the methodology implemented to model the 3D structure of the Dinantian reservoir. CS – checkshots; DEM – Digital Elevation Model; DT – sonic log; RHOB – density log; Vint – interval velocities.

Overall, the Dinantian series deepens southward. The modelled top-Dinantian surface has a maximum elevation of 122 metres in Belgium, northeast of Mons, and reaches a maximum depth of ~7,000 metres at the southern end of the study area. In the Lille-Tournai metropolitan area, where the Dinantian reservoir is exploited for its natural water resources, the structure of the Dinantian is well constrained by numerous wells (Fig. 5) and some localised outcrops (Tournai area, Belgium). Reservoir depth varies slightly and does not exceed 150 metres, which is related to the sub-tabular character of Dinantian layers (dips below 10°). Due to the shallow depth and slight dip variations, the modelled surface appears flat in 3D at the regional scale (Fig. 6). In this area, the top of the Dinantian, as well as the entire Palaeozoic substratum and the Mesozoic-Cenozoic cover, forms a gentle dome (the Melantois-Tournaisis anticline) oriented along a N100-110° axis between Lille and Tournai (Fig. 5) (e.g. Hennebert & Doremus 1997a, b; Hennebert 1998). The Melantois-Tournaisis anticline is affected by two reverse faults of limited offset, oriented along a N100-110° direction: from north to south, the Gaurain-Ramecroix Fault (GRF) and the Haubourdin Fault (HF) (or Rumes Fault in Belgium). According to previous studies (e.g. Hennebert 1998; Minguely 2007), these faults initiated during a transtensive late Vari-

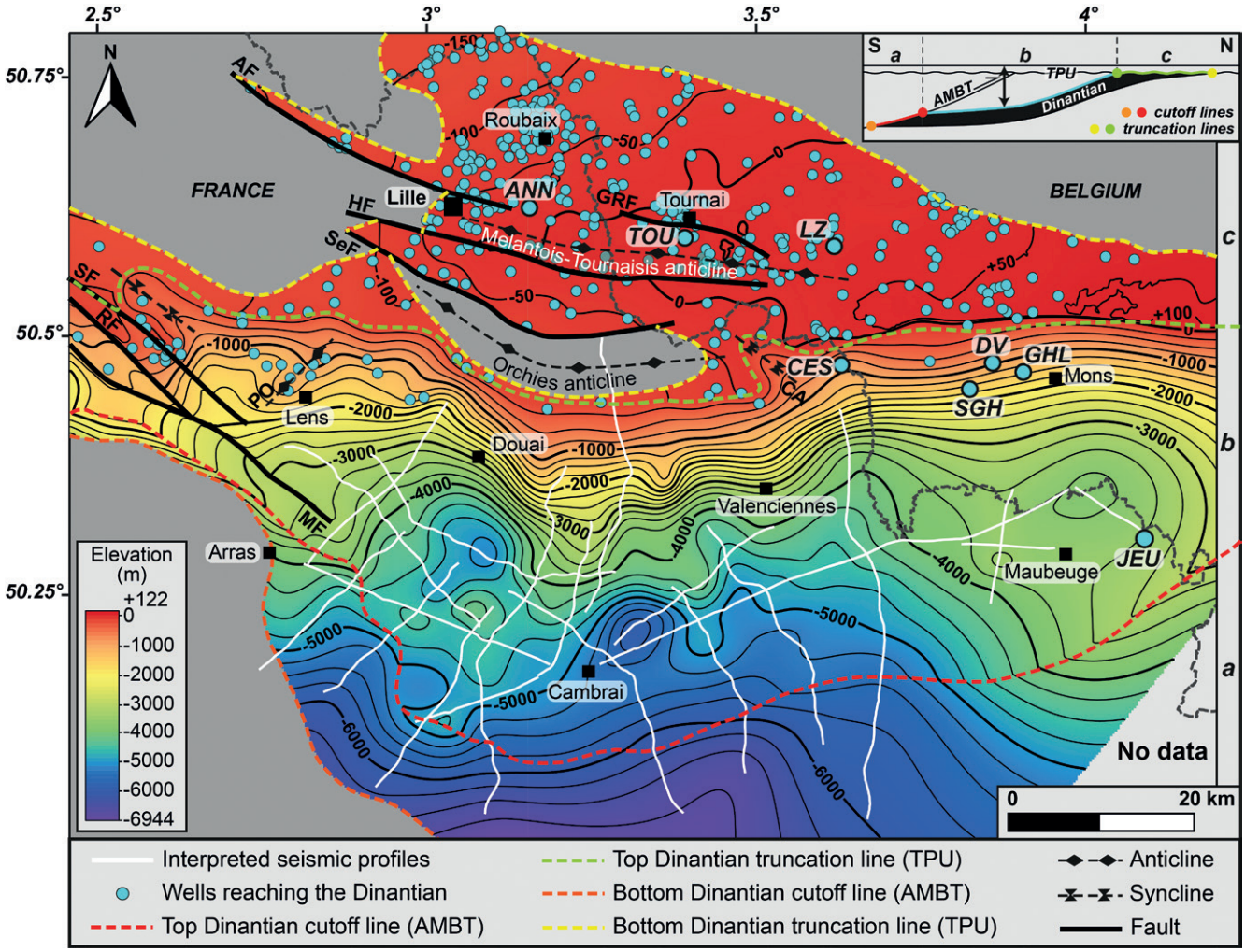

Fig. 5: Depth structural map of the top of the Dinantian, extracted from the 3D model. Grid cell size: 250 m. Faults and folds legend: AF – Armentieres Fault; CA – Chateau L'Abbaye syncline; GRF – Gaurain-Ramecroix Fault; HF – Haubourdin Fault; MF – Marqueffles Fault; PO – Poil d'Ours anticline; RF – Ruitz Fault; SF – Sains Fault; SeF – Seclin Fault. Borehole legend: same as Fig. 2a.

scan event and were reactivated as reverse faults during the Cenozoic as a result of the far-field accommodation of the Alpine-Pyrenean shortening. The general antiform would have developed as the result of this late shortening phase.

South of the Lille-Tournai metropolitan area, the monoclinal geometry of the Dinantian series rapidly deepens beneath the coal basin. According to our model, its depth ranges from 0 to approximately 3,000 metres between the northern and southern boundaries of the NPC coal district area. A major flexure is visible in the area of the NPC coal district, where the slope is steeper (10–30°) than in the rest of the region (5–10°), as shown by the tightened contour lines (Fig. 5). A slope break at the northern edge of the coal basin district is clearly apparent in 3D (top Dinantian truncation line in Fig. 6). Maximum dips ranging between 20 and 30° have been recorded near Douai and Valenciennes. This major flexure is associated to the exhumation of the Dinantian and Palaeozoic substratum directly below the Mesozoic-Cenozoic cover along the N90-120° striking Orchies anticline. This anticline is bounded to the north by the north-dipping Seclin normal fault (SeF) having a similar orientation. It is suggested that this uplift of the Brabant foreland may have been caused by the Variscan reactivation as back-thrusts of deep south-vergent Caledonian thrusts in the basement (Minguely et al. 2008).

Localised folds are noticeable in some parts of the coal basin district, such as the Chateau L'Abbaye syncline (striking N120°) and the Poil d'Ours anticline (striking N50°) (Fig. 5). At the western end of the coal district area in the Artois region (west of Lens), the Dinantian carbonate reservoir is segmented by several steeply south-dipping faults striking N130°; from north to south: the Sains Fault (SF), the Ruitz Fault (RF) and the Marqueffles Fault (MF). Seismic studies in the Artois region (Minguely 2007; Minguely et al. 2010) suggested that these faults are rooting down onto Variscan thrusts at depth and that they were formed during the late Carboniferous-Permian extensional period by negative tectonic inversion of these Variscan thrusts. A second defor-

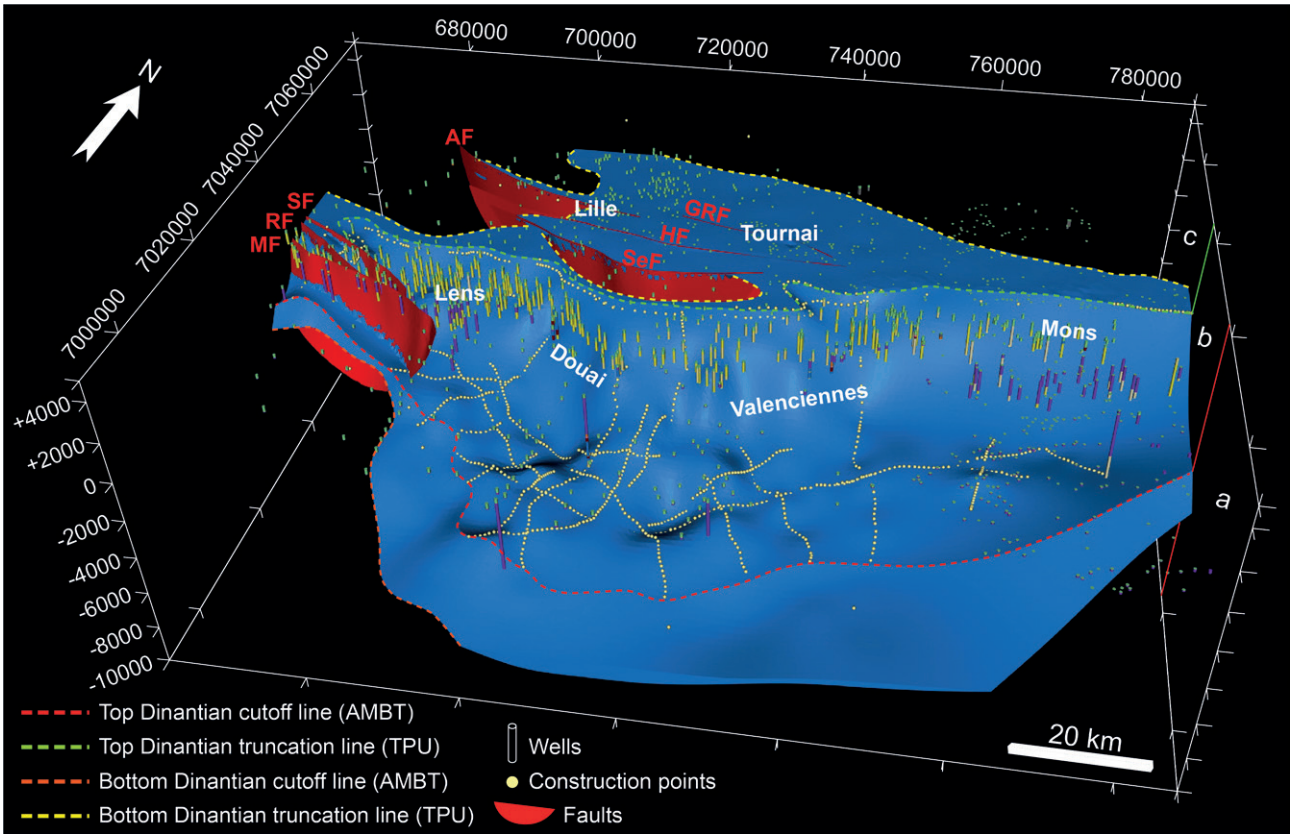

Fig. 6: 3D view of the top of the Dinantian modelled in the GeoModeller Software (grid cell size: 1,000 m, vertical exaggeration: x3). Coordinates are in French Lambert 93 and elevation values are in metres. Areas (a), (b) and (c) as well as the fault legend are defined in Fig. 5.

mation phase related to the far-field accommodation of the Alpine-Pyrenean shortening during the Tertiary would have resulted in the positive tectonic inversion of those faults as evidenced by the uplift of the Artois hills.

South of the coal district area, the Dinantian reservoir reaches depths approximately ranging from 3,000 to about 7,000 metres. The modelled geometry appears complex and irregular, especially in the Cambrai and Maubeuge areas. There, the interpretation of the deep seismic profiles revealed an intense deformation of the Dinantian series by deep Variscan thrusts. These thrusts would have a "décollement" level within the underlying Famennian shales and affected the entire para-autochthonous sequence (Laurent et al. 2021). At present-day, only the ramp-related fold structures at the hanging wall of those thrusts have been taken into account in our model, thus explaining the irregular geometry of the Dinantian series (the 3D modelling of the thrusts themselves and their implementation in the 3D model is still in progress).

Overall, in the study area, the top-Dinantian surface is structured along two main directions: N70-80° (e.g. the areas of Mons, Valenciennes, and Cambrai) and N110-130° (e.g. the area of Douai and SW of Maubeuge). Interestingly, our previous work based on the interpretation of the seismic data showed that the underlying southern Laurussian margin was structured along the same structural axes in the study area (Laurent et al. 2021), which suggests that the Devonian syn-rift prestructuration of the southern Laurussian margin had a major influence on the 3D configuration of the Variscan thrusts and of the resulting flexural behaviour of the underthrust foreland.

The 3D modelling of the base of the Dinantian reservoir shows a similar geometry and structural trends. Preliminary results suggest major thickness variations of the Dinantian reservoir in the study area. Their origin, whether sedimentary or tectonic, remains difficult to identify before the final completion of the 3D model, and are not discussed in the present paper.

Further improvements are needed to produce a final representation of the 3D geometry of the Dinantian reservoir in northern France. They will include the 3D modelling of (1) deep Variscan thrusts interpreted in seismics that are affecting the Dinantian reservoir south of the coal district area, and (2) second-order faults known in the Brabant foreland. Particular attention will be paid to the modelling of the internal structure of the coal basin, whose deformations directly affect the underlying para-autochthonous sequence, especially the Dinantian reservoir. Finally, an in-depth assessment of the uncertainties associated with the 3D modelling of the Dinantian reservoir will be carried out. A combined qualitative

and quantitative approach will help to evaluate the impact that each source of uncertainty can have on the output of the 3D modelling, whether they are associated to the borehole data (measured depth, trajectory, well logs, etc.), the seismic data (acquisition, reprocessing, resolution, horizons and faults picking, geological understanding, etc.), the time-depth conversion (velocity model, structural complexity, etc.) or the 3D modelling process itself (algorithm, resolution, data spatial distribution, geological understanding, etc.).

5. Conclusions

The 3D structural modelling of the Northern Variscan Front in northern France-southwestern Belgium, based on the integration and interpolation of data from 1,128 boreholes and 532 km of interpreted seismic reflection profiles, provides an unprecedented image of the 3D geometry of the buried Dinantian carbonate reservoir in the region. Our 3D approach highlights the main structural features of the reservoir at the regional scale and offers a first interpretation of its typical depth across the study area.

Overall, our results illustrate that the Dinantian carbonate reservoir has a general monoclinal geometry due to the flexural response of the Variscan foreland to thrust-loading. It displays an overall south- to southwestward dip underneath the NPC coal basin. We document the unprecedentedly appreciated subsurface presence of the reservoir across the territory as it extends over an area of approximately 7,675 km^2 and at least 30–40 km south of the coal district area, beneath the Ardenne Allochthonous Unit of the Northern Variscan Front. The southern limit of extension is defined by the cut-off surface of the Dinantian sequence at some major frontal and lateral ramps of the AMBT. The Dinantian reservoir is generally less than 200 m deep in the Lille metropolitan area but it reaches 1,000–3,000 m depth beneath the coal basin district and finally a maximum depth of approximately 7,000 m at the southern end of the study area. Our results document that the Dinantian reservoir is deformed along two main directions striking N70-80° and N110-130°. This structural pattern is the main result of Variscan thrusts moulded on the initial syn-rift configuration of the Laurussian margin. Subsequent deformation events (i.e. the late Carboniferous-Permian rifting as well as the Tertiary inversion phase related to the far-field accommodation of the Alpine-Pyrenean shortening) produced only localised second-order structures (i.e. Boulonnais-Artois and Melantois-Tournaisis anticlines).

The model still needs some improvements, for instance regarding the geometry of both the deep Variscan thrusts and the coal basin. Anyway, this 3D structural model provides an unprecedented representation of the regional 3D geometry of the Dinantian reservoir in northern France. Once completed, it may ultimately be used in hydrodynamic modelling studies and/or help to target specific areas of geothermal interest, prefiguring local investigations to determine the in-depth geothermal potential of the Dinantian reservoir.

6. Acknowledgements

This work is part of the PhD thesis of AL, granted by the BRGM (French Geological Survey) and the Hauts-de-France region. It also benefitted from a financial support from the TelluS Program of the CNRS/INSU. The reprocessing of the seismic profiles integrated in the database was supported by the RGF (Référentiel Géologique de la France) program of the BRGM. IHS Markit is greatly acknowledged for the permission to use the Kingdom Suite software through an academic grant to the University of Lille. The authors also thank the BRGM for providing the working licence of the GeoModeller software.

This study was also supported by the Interreg NWE Programme through the Roll-out of Deep Geothermal Energy in North-West Europe (DGE-ROLLOUT) Project (www.nweurope.eu/DGE-Rollout). The Interreg NWE Programme is part of the European Cohesion Policy and is financed by the European Regional Development Fund (ERDF).

The authors gratefully acknowledge the associate editor M. Arndt as well as the reviewers, E. Poty and an anonymous reviewer for their constructive comments on the preliminary version of this article.

7. References

Arndt, M. (2021, this issue). 3D modelling of the Lower Carboniferous (Dinantian) as an indicator for the deep geothermal potential in North Rhine-Westphalia (NRW, Germany). [Journal of Applied and Regional Geology]. *Zeitschrift der Deutschen Gesellschaft für Geowissenschaften, 172*(3), 307–324. https://doi.org/10.1127/zdgg/2021/0279

Aug, C., Chilès, J. P., Courrioux, G., & Lajaunie, C. (2005). 3D geological modelling and uncertainty: The potential-field method. In O. Leuangthong & C. V. Deutsch (Eds.), *Geostatistics Banff 2004* (pp. 145–154). Dordrecht: Springer. https://doi.org/10.1007/978-1-4020-3610-1_15

Averbuch, O., & Piromallo, C. (2012). Is there a remnant Variscan subducted slab in the mantle beneath the Paris basin? Implications for the late Variscan lithospheric delamination process and the Paris basin formation. *Tectonophysics, 558–559*, 70–83. https://doi.org/10.1016/j.tecto.2012.06.032

Averbuch, O., Mansy, J.-L., Lamarcheb, J., Lacquement, F., & Hanot, F. (2004). Geometry and kinematics of the Boulonnais fold-and-thrust belt (N France): Implications for the dynamics of the Northern Variscan thrust front. *Geodinamica Acta, 17*(2), 163–178. https://doi.org/10.3166/ga.17.163-178

Becq-Giraudon, J.-F. (1983). Synthèse structurale et paléogéographique du bassin houiller du Nord et du Pas-de-Calais. *Mémoires du Bureau de Recherches Géologiques et Minières, 123*, 1–67.

Bouroz, A. (1950). Sur quelques aspects du mécanisme de la déformation tectonique dans le bassin houiller du Nord de la France. *Annales de la Société Géologique du Nord, 70*(1), 2–55.

Bouroz, A. (1969). Le Carbonifère du Nord de la France. *Annales de la Société Géologique du Nord, 89*(1), 47–65.

Bouroz, A., Chalard, J., Dalinval, A., & Stiévenard, M. (1961). La structure du bassin houiller du Nord de la région de Douai à la frontière Belge. *Annales de la Société Géologique du Nord, 81*(1), 173–218.

Broothaers, M., Lagrou, D., Laenen, B., Harcouët-Menou, V., & Vos, D. (2021, this issue). Deep geothermal energy in the Lower Carboniferous carbonates of the Campine Basin, northern Belgium: An overview from the 1950's to 2020. [Journal of Applied and Regional Geology]. *Zeitschrift der Deutschen Gesellschaft für Geowissenschaften, 172*(3), 211–225. https://doi.org/10.1127/zdgg/2021/0285

Calcagno, P., Chilès, J. P., Courrioux, G., & Guillen, A. (2008). Geological modelling from field data and geological knowledge: Part I. Modelling method coupling 3D potential-field interpolation and geological rules. *Physics of the Earth and Planetary Interiors, 171*(1-4), 147–157. https://doi.org/10.1016/j.pepi.2008.06.013

Cazes, M., Torreilles, G., Bois, C., Damotte, B., Galdeano, A., Hirn, A., . . . Raoult, J.-F. (1985). Structure de la croute hercynienne du Nord de la France: Premiers résultats du profil ECORS. *Bulletin de la Société Géologique de France, I*(6), 925–941. https://doi.org/10.2113/gssgfbull.I.6.925

CFP – Compagnie Française de Pétrole, COPESEP – Compagnie des Pétroles du Sud-Est Parisien, RAP – Régie Autonome des Pétroles, & SNPA – Société Nationale des Pétroles d'Aquitaine. (1965). Contribution à la connaissance des bassins paléozoïques du Nord de la France. *Annales de la Société Géologique du Nord, 85*(1), 273–281.

Chantraine, J., Autran, A., Cavelier, C., Alabouvette, B., Barféty, J.-C., Cecca, F., . . . Ternet, Y. (2003). *Carte géologique de la France à l'échelle du millionième*. Orléans: BRGM.

Chilès, J. P., Aug, C., Guillen, A., & Lees, T. (2004). Modelling the geometry of geological units and its uncertainty in 3D from structural data: The potential-field method. In R. Dimitrakopoulos, & S. Ramazan (Eds.), *Orebody Modelling and Strategic Mine Planning* (pp. 313–320). Spectrum Series, 14. Carlton, Victoria: Australasian Institute of Mining and Metallurgy.

Coen-Aubert, M., Groessens, E., & Legrand, R. (1980). Les formations paléozoïques des sondages de Tournai et de Leuze. *Bulletin de la Société Belge de Géologie, 89*(4), 241–275.

COPESEP (1965). *Rapport de fin de sondage Jeumont-Marpent n°1 – "JEU. 1". N°14.3037* (23 pp.).

Delmer, A. (1977). Le bassin du Hainaut et le sondage de St-Ghislain. *Geological Survey of Belgium*. *Professional Paper, 6*(143), 1–12.

Delmer, A. (1982). Recherches géothermiques en Belgique. *Annales de la Société Géologique du Nord, 102*, 87–88.

Delmer, A. (1997). Structure tectonique du bassin houiller du Hainaut. *Annales de la Société Géologique du Nord, 5*(2), 7–15.

Delmer, A. (2003). La structure tectonique transfrontalière entre les bassins houillers de Valenciennes (France) et du Hainaut belge. *Geologica Belgica, 6*(3–4), 171–180.

Delmer, A., Dusar, M., & Delcambre, B. (2001). Upper Carboniferous lithostratigraphic units (Belgium). *Geologica Belgica, 4*(1–2), 95–103.

De Putter, T. (1995). Etude sédimentologique de la Grande brèche viséenne ("V3a") du bassin de Namur-Dinant. *Mémoires pour Servir à l'Explication des Cartes Géologiques et Minières de la Belgique, 40*, 1–272.

De Putter, T., Groessens, E., & Herbosch, A. (1991). Le "V3a" anhydritique du sondage de Saint-Ghislain (150E387, Province du Hainaut, Belgique): Description macroscopique et structures sédimentaires. *Geological Survey of Belgium*. *Professional Paper, 6*(250), 1–22.

De Putter, T., Rouchy, J.-M., Herbosch, A., Keppens, E., Pierre, C., & Groessens, E. (1994). Sedimentology and palaeo-environment of the Upper Visean anhydrite of the Franco-Belgian Carboniferous basin (Saint-Ghislain borehole, southern Belgium). *Sedimentary Geology, 90*(1–2), 77–93. https://doi.org/10.1016/0037-0738(94)90018-3

Farquharson, N., Schubert, A., & Steiner, U. (2016). Geothermal energy in Munich (and beyond). A geothermal city case study. *Geothermal Resources Council*. *Transactions, 40*, 189–196.

Franke, W. (2000). The mid-European segment of the Variscides: Tectonostratigraphic units, terrane boundaries and plate tectonic evolution. *Special Publication – Geological Society of London, 179*(1), 35–61. https://doi.org/10.1144/GSL.SP.2000.179.01.05

Franke, W., Cocks, L. R. M., & Torsvik, T. H. (2017). The Palaeozoic Variscan oceans revisited. *Gondwana Research, 48*, 257–284. https://doi.org/10.1016/j.gr.2017.03.005

Groessens, E., Conil, R., & Hennebert, M. (1982). Le Dinantien du sondage de Saint-Ghislain. *Mémoires pour Servir à l'Explication des Cartes Géologiques et Minières de la Belgique, 22*, 1–137.

Hance, L., Poty, E., & Devuyst, F.-X. (2001). Stratigraphie sequentielle du Dinantien type (Belgique) et corrélation avec le Nord de la France (Boulonnais, Avesnois). *Bulletin de la Société Géologique de France, 172*(4), 411–426. https://doi.org/10.2113/172.4.411

Hance, L., Poty, E., & Devuyst, F.-X. (2006a). Tournaisian. In L. Dejonghe (Ed.), *Current status of chronostratigraphic units named from Belgium and adjacent areas. Geologica Belgica, 9*(1–2), 47–53.

Hance, L., Poty, E., & Devuyst, F.-X. (2006b). Viséan. In L. Dejonghe (Ed.), *Current status of chronostratigraphic units named from Belgium and adjacent areas. Geologica Belgica, 9*(1–2), 55–62.

Hennebert, M. (1998). L'anticlinal faillé du Mélantois-Tournaisis fait partie d'une "structure en fleur positive" tardi-varisque. *Annales de la Société Géologique du Nord, 6*(2), 65–78.

Hennebert, M., & Doremus, P. (1997a). Antoing-Leuze. Carte géologique de Wallonie. Echelle 1/25.000. *Notice Explicative, 37*(7–8), 1–74.

Hennebert, M., & Doremus, P. (1997b). Hertain-Tournai. Carte géologique de Wallonie. Echelle 1/25.000. *Notice Explicative., 37*(5–6), 1–66.

Khatir, A., Mansy, J.-L., & Meilliez, F. (1988). Structures et déformation dans l'allochtone ardennais en Avesnois (Nord). *Annales de la Société Géologique du Nord, 108*(2–3), 73–83.

Lacquement, F. (2001). L'Ardenne varisque. Déformation progressive d'un prisme sédimentaire pré-structuré; de l'affleurement au modèle de chaîne. *Société Géologique du Nord*. *Publication, 29*, 1–285.

Lacquement, F., Mansy, J.-L., Hanot, F., & Meilliez, F. (1999). Retraitement et interprétation d'un profil sismique pétrolier méridien au travers du Massif paléozoïque ardennais (Nord de la France). *Comptes Rendus de l'Académie des Sciences Paris*. *Sciences de la Terre et des Planètes, 329*(7), 471–477.

Lajaunie, C., Courrioux, G., & Manuel, L. (1997). Foliation fields and 3D cartography in geology: Principles of a method based on potential interpolation. *Mathematical Geology, 29*(4), 571–584. https://doi.org/10.1007/BF02775087

Laurent, A., Averbuch, O., Beccaletto, L., Graveleau, F., Lacquement, F., Capar, L., … Marc, S. (2021): 3-D structure of the Variscan Thrust Front in northern France: New insights from seismic reflection profiles. *Tectonics, 40*(7), e2020TC006642. https://doi.org/10.1029/2020TC006642

Le Gall, B. (1994). Deformation of the Nord-Pas-de-Calais Carboniferous coalfield (France) in the Variscan frontal tectonic pattern. In A. Mascle (Ed.), Hydrocarbon and petroleum geol-

ogy of France. *Special Publication of the European Association of Petroleum Geoscientists, 4*, 379–398.
Licour, L. (2012). Relations entre la géologie profonde et le comportement hydrogéologique du réservoir géothermique du Hainaut (Belgique) – Caractérisation de l'aquifère dans la région de Saint-Ghislain. *Doctoral dissertation Université de Mons (Belgium)* (372 pp.).
Mansy, J.-L., & Lacquement, F. (2006). Contexte géologique régional: L'Ardenne paléozoïque (Nord de la France et Sud de la Belgique). *Géologie de la France, 1–2*, 7–13.
Mansy, J.-L., & Meilliez, F. (1993). Eléments d'analyse structurale à partir d'exemples pris en Ardenne-Avesnois. *Annales de la Société Géologique du Nord, 2*(2), 45–60.
Mansy, J.-L., Lacquement, F., Meilliez, F., Hanot, F., & Everaerts, M. (1997). Interprétation d'un profil sismique pétrolier, sur le méridien de Valenciennes (Nord de la France). *Aardkundige Mededelingen, 8*, 127–129.
Mansy, J.-L., Everaerts, M., & De Vos, W. (1999). Structural analysis of the adjacent Acadian and Variscan fold belts in Belgium and northern France from geophysical and geological evidence. *Tectonophysics, 309*(1–4), 99–116. https://doi.org/10.1016/S0040-1951(99)00134-1
Mansy, J.-L., Manby, G. M., Averbuch, O., Everaerts, M., Bergerat, F., Van Vliet-Lanoe, B., . . . Vandycke, S. (2003). Dynamics and inversion of the Mesozoic basin of the Weald–Boulonnais area: Role of basement reactivation. *Tectonophysics, 373*(1–4), 161–179. https://doi.org/10.1016/S0040-1951(03)00289-0
Marsden, D. (1989). Layer cake depth conversion, Part I. *The Leading Edge, 8*(1), 10–14. https://doi.org/10.1190/1.1439561
Maxelon, M., Renard, P., Courrioux, G., Brändli, M., & Mancktelow, N. (2009). A workflow to facilitate three-dimensional geometrical modelling of complex poly-deformed geological units. *Computers & Geosciences, 35*(3), 644–658. https://doi.org/10.1016/j.cageo.2008.06.005
McInerney, P., Guillen, A., Courrioux, G., Calcagno, P., & Lees, T. (2005). Building 3D geological models directly from the data? A new approach applied to Broken Hill, Australia. *Digital Mapping Techniques, 2005*, 119–130.
Meilliez, F. (2019). La Faille du Midi, mythe et réalités. *Annales de la Société Géologique du Nord, 26*(2), 13–32.
Meilliez, F., & Mansy, J.-L. (1990). Déformation pelliculaire différenciée dans une série lithologique hétérogène: Le Dévono-Carbonifère de l'Ardenne. *Bulletin de la Société Géologique de France,* VI(1), 177–188. https://doi.org/10.2113/gssgfbull.VI.1.177
Meilliez, F., André, L., Blieck, A., Fielitz, W., Goffette, O., Hance, L., . . . Verniers, J. (1991). Ardenne-Brabant. *Sciences Géologiques. Bulletin, 44*(1–2), 3–29. https://doi.org/10.3406/sgeol.1991.1864
Minguely, B. (2007). Caractérisation géométrique 3-D de la couverture sédimentaire méso-cénozoïque et du substratum varisque dans le Nord de la France: Apports des données de sondages et des données géophysiques. *Doctoral dissertation Université de Lille* (231 pp.).
Minguely, B., Folens, L., Averbuch, O., & Vendeville, B. C. (2008). Formation of deep-seated triangle zones by interaction between two orogenic thrust fronts having opposite vergence: Structural evidence from the Caledonian-Variscan system in Northern France and preliminary analogue modelling. *Bollettino di Geofisica Teorica ed Applicata, 49*(2), 242–246.
Minguely, B., Averbuch, O., Patin, M., Rolin, D., Hanot, F., & Bergerat, F. (2010). Inversion tectonics at the northern margin of the Paris basin (northern France): New evidence from seismic profiles and boreholes interpolation in the Artois area. *Bulletin de la Société Géologique de France, 181*(5), 429–442. https://doi.org/10.2113/gssgfbull.181.5.429
Moulouel, H. (2008). Caractérisation cartographique d'une différenciation verticale et horizontale de la. déformation: Application à la couverture sédimentaire de la plate-forme ardennaise. *Doctoral dissertation Université de Lille* (205 pp.).
Oncken, O., von Winterfeld, C., & Dittmar, U. (1999). Accretion of a rifted passive margin: The Late Paleozoic Rhenohercynian fold and thrust belt (Middle European Variscides). *Tectonics, 18*(1), 75–91. https://doi.org/10.1029/98TC02763
Oncken, O., Plesch, A., Weber, J., Ricken, W., & Schrader, S. (2000). Passive margin detachment during arc-continent collision (Central European Variscides). *Special Publication – Geological Society of London, 179*(1), 199–216. https://doi.org/10.1144/GSL.SP.2000.179.01.13
Pharaoh, T., Jones, D., Kearsey, T., Newell, A., Abesser, C., Randles, T., . . . Kendall, R. (2021, this issue). Early Carboniferous limestones of southern and central Britain: Characterisation and preliminary assessment of deep geothermal prospectivity. [Journal of Applied and Regional Geology]. *Zeitschrift der Deutschen Gesellschaft für Geowissenschaften, 172*(3), 227–249. https://doi.org/10.1127/zdgg/2021/0282
Poty, E., Hance, L., Lees, A., & Hennebert, M. (2001). Dinantian lithostratigraphic units (Belgium). *Geologica Belgica, 4*(1–2), 69–94.
Pracht, M., Rogers, R., & McConnell, B. J. (2021, this issue). Mississippian (Dinantian) of Ireland and its geothermal potential. [Journal of Applied and Regional Geology]. *Zeitschrift der Deutschen Gesellschaft für Geowissenschaften, 172*(3), 267–292. https://doi.org/10.1127/zdgg/2021/0280
Raoult, J.-F. (1986). Le front varisque du Nord de la France d'après les profils sismiques, la géologie de surface et les sondages. *Revue de Géologie Dynamique et de Géographie Physique, 27*(3–4), 247–268.
Raoult, J.-F., & Meilliez, F. (1987). The Variscan Front and the Midi Fault between the Channel and the Meuse river. *Journal of Structural Geology, 9*(4), 473–479. https://doi.org/10.1016/0191-8141(87)90122-2
Rouchy, J. M., Pierre, C., Groessens, E., Monty, C., Laumondais, A., & Moine, B. (1986). Les évaporites pré-permiennes du segment varisque franco-belge: Aspects paléogéographiques et structuraux. *Bulletin de la Société Belge de Géologie, 95*(2–3), 139–149.
Rouchy, J. M., Laumondais, A., & Groessens, E. (1987). The Lower Carboniferous (Visean) evaporites in northern France and Belgium: Depositional, diagenetic and deformational guides to reconstruct a disrupted evaporitic basin. In T. M. Peryt (Ed.), *Evaporite basins. Lecture Notes in Earth Sciences, 13(1), 31–67*. https://doi.org/10.1007/BFb0010099
Shail, R. K., & Leveridge, B. E. (2009). The Rhenohercynian passive margin of SW England: Development, inversion and extensional reactivation. *Comptes Rendus Geoscience, 341*(2–3), 140–155. https://doi.org/10.1016/j.crte.2008.11.002

Manuscript received: 02.03.2021
Revisions required: 21.04.2021
Revised version received: 14.05.2021
Accepted for publication: 18.08.2021